Evaluation of Chemical and Nano-Based Biocides for Controlling Microbial Corrosion of Carbon Steel Pipes During Hydrostatic Testing

Mina Rezapour*[1], Ali Hassanzadeh[2], Nima Shaykh-Baygloo[3]

[1] MSc in Physical Chemistry, Faculty of Chemistry, Urmia University, Urmia, Iran. mi.rezapour@urmia.ac.ir

[2] Associate Professor, Department of Analytical-Physical and Applied Chemistry, Faculty of Chemistry, Urmia University, Urmia, Iran. a.hassanzadeh@urmia.ac.ir

[3] Associate Professor, Department of Biology, Faculty of Science, Urmia University, Urmia, Iran, n.baygloo@urmia.ac.ir

Abstract:

Sulfate-reducing bacteria (SRB) are anaerobic microorganisms that significantly contribute to microbial corrosion, especially in metallic infrastructures such as gas and oil pipelines. This problem becomes more critical during hydrostatic testing, when SRB-contaminated water accelerates corrosion in carbon steel pipes. In this study, water samples from deep and surface wells were analyzed using 16S rRNA gene sequencing, confirming dominant SRB strains such as *Clostridium perfringens* (UGWCp01, UGWCp04) and *Paraclostridium* (UGWPc02). To mitigate SRB activity, several chemical biocides (glutaraldehyde, isothiazolin, a bronopol–isothiazolin mix) and silver nanoparticles were tested at equal final dosages in contaminated water in contact with carbon steel specimens under anaerobic conditions. Corrosion inhibition was evaluated using potentiodynamic polarization (LSV/Tafel) and electrochemical impedance spectroscopy (EIS), and surface changes were characterized by SEM and XRD after long-term immersion simulating hydrostatic exposure. Silver nanoparticles produced the lowest corrosion current densities and the highest impedance responses, consistent with markedly reduced pitting and sulfide deposits. Overall, AgNPs showed the strongest antimicrobial and corrosion-inhibiting performance, indicating a promising alternative for protecting steel during SRB-driven hydrostatic testing.

Keywords: Carbon Steel, Sulfate-Reducing Bacteria, Microbial Corrosion, Chemical Biocides, Silver Nanoparticles

1. Introduction

Microbial corrosion is a major category of material degradation and accounts for a substantial portion of corrosion-related economic losses in industrial systems [1–4] with estimates indicating that nearly 20% of total corrosion costs originate from microbial activity [5–7]. The initiation of microbiologically influenced corrosion (MIC) is strongly associated with biofilm formation, where microbial communities (particularly SRB), attach to metal surfaces and accelerate the deterioration of ferrous alloys under anaerobic conditions [8, 9].

Hydrostatic testing is an essential step prior to commissioning gas pipelines; however, the prolonged contact between carbon steel and the water used in this test creates a suitable environment for SRB proliferation and MIC development. Despite the widespread industrial use of hydrostatic testing, very few studies have examined the actual microbial composition of field water used in this process or its contribution to SRB-driven corrosion. This issue is particularly relevant in northwestern Iran, where several pipeline failures have been associated with microbial contamination, yet the dominant SRB species in these waters remain insufficiently characterized [10, 11].

Although biocides such as ozone, UV/peracetic acid and chlorine have been applied to suppress microbial activity in water systems [12–15], their use in pipeline operations faces considerable limitations. Chlorine, for instance, may intensify metal corrosion and shows poor efficacy against resistant SRB spores such as *Clostridium* [15, 16]. Consequently, the development of more effective and stable alternatives for MIC control is necessary.

In recent years, silver nanoparticles (AgNPs) have attracted significant attention as antimicrobial agents; however, most existing studies have focused on *Desulfovibrio* species under synthetic laboratory conditions. Little is known about the performance of AgNPs against the field-dominant SRB communities, particularly *Clostridium* and *Paraclostridium*, nor about their comparative effectiveness relative to multiple industrial biocides under long-term, anaerobic, hydrostatic-like conditions. This gap represents the central research problem addressed in this study.

To fill this gap, SRB species present in real hydrostatic-testing water were isolated and identified using PCR and sequencing. Carbon steel coupons were then exposed to this contaminated water under anaerobic conditions and three widely used industrial biocides (alongside AgNPs) were evaluated over a 40-day immersion period. Corrosion behavior and mechanisms were assessed using LSV and EIS, while XRD and SEM were applied to characterize corrosion products and surface morphology.

The central hypothesis of this study is that AgNPs, owing to their strong antibiofilm and antimicrobial activity, provide superior MIC inhibition compared with conventional chemical biocides. The objectives are: (i) to identify the dominant SRB species in real hydrostatic-testing water; (ii) to investigate the corrosion behavior of SRB-exposed carbon steel under anaerobic conditions and (iii) to compare the performance of AgNPs with three industrial biocides in suppressing MIC.

By integrating field-isolated SRB communities with advanced electrochemical and surface-analysis techniques, this study provides one of the first comprehensive evaluations of AgNP performance against *Clostridium*-dominated MIC in hydrostatic-testing environments.

2. Materials and Methods

This study involved sampling groundwater and surface water to isolate bacteria responsible for microbial corrosion, aiming to evaluate the effects of various chemical biocides on these bacteria and, consequently, to prevent microbial corrosion of steel pipes. Sampling sites for groundwater and surface water were chosen from the water-rich regions of Urmia, a city in western Iran and a crucial area for transmitting long-distance gas pipelines, where corrosion control of steel pipes is essential (Table 1). Multiple samples were collected from various surface and groundwater sources commonly used in hydrostatic testing by the gas company, adhering to standard water sampling protocols.

2.1. Sampling strategy

Five water sources commonly used by the regional gas company for hydrostatic testing in the Urmia operational corridor were purposively selected to represent field-relevant SRB-contaminated test waters rather than to estimate province-wide microbial variability. The subsequent MIC experiments were therefore designed to benchmark biocide performance under these real hydrostatic-water conditions.

2.2. Water Sampling Standards

Sampling containers were pre-autoclaved and thoroughly sterilized. Disposable gloves were used during sampling, and hands were disinfected with alcohol. Sample containers were opened only once for sample collection. To ensure the presence of anaerobic SRB, samples were taken from wells or deep wells with low to moderate turbidity, from a depth of 20 cm to target anaerobic bacteria. Samples were tested within 24 hours of collection, and locations away from household wastewater, factories, or polluted areas were chosen, with water samples taken at a temperature of 25°C.

Samples were cultured on tryptose sulfite cycloserine (TSC) agar to detect SRB contamination. After culturing, the samples underwent PCR sequencing to accurately identify the bacterial strains present.

Carbon steel gas pipeline coupons (API-5L-B) were prepared for corrosion studies and biological observations to examine the impact of various chemical biocides on these bacteria. All coupons were rinsed with deionized water and given a final ultrasonic wash with alcohol. Chemical biocides, including glutaraldehyde, isothiazolin, and a mixture of isothiazolin and bronopol, were obtained from the Iranian company Energy Chemical Semnan. A colloidal silver nanoparticle solution was synthesized by chemically reducing $AgNO_3$ with $NaBH_4$ in the presence of CTAB as a stabilizer.

2.3. Identification and Isolation of SRB Bacteria Including Clostridium and Paraclostridium Species

Given the high abundance of sulfate-reducing bacteria (SRB) and time limitations, we focused on the dominant spore-forming SRB group, namely Clostridium/Paraclostridium, as the indicator organism. A membrane filtration method and TSC agar medium, specifically suited for low-turbidity water samples with low bacterial density, were used to isolate and identify this bacterium. Water samples were treated at 75°C for 10 minutes shortly after collection to isolate *Clostridium* spores, ensuring only heat-resistant strains, such as *Clostridium perfringens*, were retained. Ten milliliters of each sample were filtered twice, with the filters placed onto freshly prepared TSC agar plates (Oxoid, Hampshire, United Kingdom) and incubated in an anaerobic jar at 37°C for 48 hours.

2.4. PCR Procedure for Bacteria Cultured on TSC Agar

DNA was extracted from fresh bacterial cultures using the boiling method. The extracted DNA quality was assessed using a NanoDrop spectrophotometerM. In order to identify bacterial strains, PCR was performed using universal primers 27F (5′-AGAGTTTGATCCTGGCTCAG-3′) and 1492R (5′-GGTTACCTTGTTACGACTT-3′) designed for the 16S rRNA gene in a 50 μL volume containing 5 μL genomic DNA, 1.5 *mM* MgCl2, 0.2 *mM* of each dNTP, 0.4 μM of each primer, 20 *mM* Tris-HCl, 50 *mM* KCl, 2.5 units of Smar Taq DNA polymerase (Sinaclon, Iran), and sterile double-distilled water. PCR temperature conditions included 95°C for 5 minutes, followed by 40 cycles of 30 seconds at 95°C, 30 seconds at 55°C, and 30 seconds at 72°C, with a final 7 minutes extension at 72°C. The PCR products were analyzed by electrophoresis using 1% agarose gel and TBE buffer, and sequenced by Macrogen Company (South Korea). Finally, the obtained sequences were analyzed using the BLAST tool in the NCBI database (http://blast.ncbi.nlm.nih.gov/Blast.cgi). It is noted that the PCR mixture without extracted DNA was used as a negative control.

2.5. Preparation of Standard Concentrations of Isothiazolin, Glutaraldehyde, and Isothiazolin-Bronopol Biocides

The tested biocides (isothiazolinone-based, glutaraldehyde-based and isothiazolinone/bronopol formulations) were commercial ready-to-use products; therefore, no biocide synthesis was performed in this work. Working solutions were freshly prepared by diluting each commercial product in sterile thioglycollate medium to a final product dosage of 200 $mg{\cdot}L^{-1}$ (200 ppm) using $C_1V_1=C_2V_2$, where C_1 denotes the as-received commercial stock concentration. This dosage was selected as a field-relevant shock/slug dose within the commonly recommended range for SRB control (25–200 *ppm*) [17]. The diluted biocides were added at the start of exposure to the inoculated anaerobic medium and maintained throughout the 40-day immersion period. Since these are proprietary industrial formulations, they are reported by chemical family/active type, while efficacy is benchmarked by identical final dosage and corrosion response.

2.6. Synthesis of Silver Nanoparticles

To prepare silver nanoparticles, 0.00337 *g* of silver nitrate was added to 30 *mL* of water or ethanol, and stirred on a magnetic stirrer. A stabilizer (CTAB) solution was prepared by dissolving 1.6 *g* in 500 *mL* of water, and 10 *mL* of this solution was added. Sodium borohydride, equal in molarity to silver nitrate, was used to reduce silver ions to metallic silver. A yellow color appeared at the end of the reaction, indicating the reduction of silver ions. The resulting AgNP suspension was used for antimicrobial testing

2.7. Corrosion Testing of Steel Coupons in the Presence and Absence of Biocides

Five sterilized glass containers were autoclaved after isolating and culturing the target bacteria, performing PCR, preparing antimicrobial solutions, and preparing steel coupons. To investigate the corrosion of steel coupons, five test tubes filled with thioglycollate liquid medium were autoclaved. After inoculating the bacterial strains in the thioglycollate medium, a piece of API-5L-B carbon steel was added to each of the tubes. Different biocides including isothiazolinone, glutaraldehyde, isothiazolinone-bronopol mixture, and silver nanoparticle solution were placed separately in four tubes. The fifth tube was considered a negative control without biocide. Then, all tubes were placed in an anaerobic jar in the dark for 40 days.

After 40 days, steel pieces were removed and cut into 1×1 cm squares in the lab for scanning electron microscopy (SEM) imaging to examine and compare corrosion types and levels on the steel surface. Solutions in the containers were dried, and the resulting deposits were collected and evaluated by X-ray diffraction (XRD) for deposit analysis. Results were interpreted using Xpert High Score Plus software.

2.8. Electrochemical measurements

Potentiodynamic polarization (LSV/Tafel), cyclic voltammetry (CV) and electrochemical impedance spectroscopy (EIS) were performed to assess MIC mitigation in a conventional three-electrode cell with carbon steel as the working electrode, a saturated calomel electrode (SCE) as the reference electrode, and a platinum counter electrode. The electrolyte was the same anaerobic SRB-inoculated thioglycollate medium used in the 40-day immersion experiments and contained the corresponding biocide dosage; thus, all electrochemical measurements were conducted directly in the original SRB medium without transferring the coupons to a standardized electrolyte.

EIS spectra were fitted to an appropriate equivalent circuit using commercial impedance analysis software and the goodness of fit was evaluated by χ^2 and residual analysis. Although the semicircles were depressed, the fitting quality was acceptable for comparative extraction of *Rs*, *Rct*, and *Cdl/CPE* across all treatments.

The corrosion inhibition efficiency of each treatment was calculated from the polarization curves using the corrosion current density (*i_corr*), according to **Eq. (1)**.

$$Yield\% = \frac{R_{ct}(inhibitor) - R_{ct}(blank)}{R_{ct}(blank)} * 100 \qquad (1)$$

where $i_{corr,blank}$ and $i_{corr,biocide}$ are the corrosion current densities measured in the SRB-inoculated medium without and with biocide, respectively.

3. Results and Discussion

3.1. Bacterial Culture and Gene Registration

Five water samples collected from various locations in West Azerbaijan Province were investigated for the presence of the anaerobic bacterium *Clostridium perfringens*. Using TSC agar medium and the membrane filter method, *Clostridium perfringens* was confirmed in four samples (Figure 1).

After observing black colonies on the TSC agar medium, DNA extraction, PCR analysis, and sequencing were conducted to identify the bacterial strains more accurately. The study revealed that two isolated strains were identified as *Clostridium perfringens* strains (UGWCp01 and UGWCp04), while one strain was identified as a *Paraclostridium* sp. strain (UGWPc02). The 16S rRNA gene sequences for UGWCp01, UGWPc02 and UGWCp04 are accessible in the GenBank nucleotide database under accession numbers MN955291, MN955299 and MN955298, respectively.

3.2. Corrosion Tests on Steel Coupons in the Presence and Absence of Biocides

Steel coupons, cut and polished, were exposed to contaminated water with various chemical biocides, including isothiazolin, glutaraldehyde, a mixture of isothiazolin and bronopol, silver nanoparticles, and a control sample without biocide. Visual observations yielded the following results:

Container 1 containing isothiazolinone biocide showed no blackening and only slight turbidity, with the formation of iron hydroxide precipitates observed. Container 2 containing glutaraldehyde biocide showed black iron hydroxide deposits and closely resembled the control sample. Container 3, containing a combination of isothiazolinone and bronopol biocides, did not show blackening of the solution, formed iron hydroxide with slight turbidity, and exhibited the highest transparency compared to the previous two samples. Container 4, containing antimicrobial solution of silver nanoparticles, unlike chemical biocide samples, exhibited no foul odor from microbial activity or sulfur compounds and had physical properties resembling clean water. Additionally, it showed the least corrosion of the steel piece among samples containing biocides. Container 5, the control sample, appeared as a completely black solution containing black iron deposits, likely iron sulfide. The containers with these solution residues are shown in Figure 2.

3.3. XRD Pattern Analysis

The XRD patterns of the collected sediments exhibited low-intensity peaks with considerable background noise, indicating predominantly amorphous and/or poorly crystalline deposits.

Therefore, phase identification was performed cautiously using HighScore Plus and ICDD reference patterns, and the assigned phases should be regarded as indicative.

In the AgNP-treated sample, detectable crystalline phases were mainly iron oxides/oxyhydroxides (e.g., Fe_2O_3 and FeO(OH)) with minor sulfate-containing products, while no distinct crystalline iron sulfide peaks were detected within the XRD detection limit. This suggests a markedly reduced sulfide deposition compared with glutaraldehyde and blank conditions.

In contrast, glutaraldehyde and control samples showed clear sulfide-related phases (e.g., FeS/Fe_3S_4-type reflections), consistent with the visually observed black deposits. Overall, the XRD trends are interpreted together with SEM and visual inspection to infer SRB activity and MIC severity (Figure 3).

3.4. SEM Analysis of Samples

Scanning electron microscope (SEM) images of the steel sample surfaces are presented in Figure 4, revealing the following observations. Most samples displayed pitting corrosion to varying degrees. This type of corrosion often occurs in samples protected by a thin oxide layer or biofilm, where chloride ions in the environment locally break down the film, accelerating metal degradation through pit formation. The sample containing silver nanoparticle biocide showed minimal pitting corrosion. In the isothiazolin and bronopol mixture sample, slight pitting with small pits was observed, while the isothiazolin biocide sample exhibited more pitting, with some porous regions. The glutaraldehyde sample had a bacterial biofilm on the metal surface, with porous pitting corrosion. The control sample displayed the most pronounced pitting corrosion, with larger pits. Biofilm formation in the glutaraldehyde-treated sample likely reflects stress-induced aggregation and enhanced surface colonization, which promotes localized corrosion. Unlike the isothiazolin, isothiazolin-bronopol mixture and silver nanoparticle biocides, glutaraldehyde failed to eliminate bacteria, instead creating stress conditions that encouraged biofilm formation.

3.5. Potentiodynamic Polarization (LSV/Tafel), Cyclic Voltammetry (CV), and Electrochemical Impedance Spectroscopy (EIS)

Figure 5a shows the LSV polarization comparison plot, indicating that the corrosion potential of the silver nanoparticle-coated steel shifts to more positive values than the other conditions. Table 2 presents the results of fitting the steel samples' polarization plots using the Butler–Volmer equation. Figure 5b presents an additional potentiodynamic polarization (LSV/Tafel) comparison. The AgNP-treated sample shows the lowest corrosion current density (icorr) and a nobler corrosion potential relative to the chemical biocides and blank.

CV was used to assess interfacial electrochemical behavior under different biocide treatments. The CV-derived parameters are summarized in Table 3, and the results are consistent with the polarization and EIS trends.

The Nyquist and Bode plots are presented in Figure 5c and 5d. The fitted EIS parameters are summarized in Table 4.

3.6. Biocide inhibition efficiency based on polarization curves

The resulting efficiencies are summarized in Table 5. All biocides significantly reduced *i_corr* relative to the SRB-inoculated blank. The isothiazolinone/bronopol formulation and glutaraldehyde provided the highest polarization-based inhibition efficiencies (approximately 75.7% and 74.5%, respectively), followed by AgNPs (≈67.3%), whereas isothiazolinone alone afforded only modest protection (≈24.9%). These results confirm that, under the present anaerobic MIC conditions, all three industrial formulations and AgNPs act as effective inhibitors compared with the uninhibited SRB medium, but the single-component isothiazolinone dose was insufficient to fully suppress SRB-driven corrosion. The inhibition efficiencies derived from LSV are presented in Table 5.

It should be emphasized that the inhibition efficiency derived from LSV primarily reflects short-term corrosion suppression at the time of measurement and should not be interpreted as a direct antimicrobial killing efficiency. Therefore, the relatively high LSV-based value observed for glutaraldehyde likely represents a transient electrochemical effect, whereas its long-term ability to control SRB biofilm formation and MIC under prolonged anaerobic exposure appears comparatively limited. Accordingly, the overall performance assessment in this study is based on the convergence of LSV, EIS (*Rct*), and surface evidence rather than a single electrochemical metric.

Lastly, Nyquist plots (Figure 5c) indicate that the AgNP-treated sample exhibits the highest *Rct*, whereas the glutaraldehyde and blank samples show the lowest *Rct*, confirming insufficient MIC suppression by glutaraldehyde. Figure 5d presents the Bode plot for all samples.

The fitted EIS parameters (Figure 5e) are summarized in Table 4. The AgNP-treated sample exhibited the highest *Rct* and the lowest interfacial capacitance, indicating the most effective suppression of charge-transfer processes associated with SRB-driven MIC, whereas the glutaraldehyde and blank conditions showed the lowest *Rct* values.

3.7. Discussion

The present study evaluated the efficacy of various chemical biocides in mitigating microbiologically induced corrosion (MIC) on steel coupons exposed to contaminated water. The findings revealed significant differences in the performance of each biocide, particularly highlighting the superior effectiveness of silver nanoparticles over traditional chemical biocides such as isothiazolin and glutaraldehyde.

The visual inspection of steel coupons after exposure to contaminated water indicated distinct outcomes based on the biocide used. The silver nanoparticle-treated samples exhibited the least corrosion, maintaining properties akin to clean water and avoiding foul odors associated with microbial activity. This finding aligns with the observations made by other researchers, such as [18, 19], who reported that silver nanoparticles effectively inhibited the growth of SRB, thus reducing corrosion rates significantly.

Beyond AgNPs, several nano-biocides have been explored for SRB-related MIC control. Recent studies indicate that ZnO nanoparticles and Cu-based nanomaterials can reduce SRB growth, biofilm coverage, and MIC severity on carbon steel, although their performance varies with salinity, sulfide level, and particle surface chemistry. In particular, ZnO has shown measurable MIC mitigation under anaerobic SRB exposure, while Cu-containing and Cu–Ag hybrid systems have demonstrated strong antibiofilm action against SRB biofilms. These reports suggest that Ag-,Cu- and Zn-based nanomaterials form a promising but chemistry-sensitive toolbox for hydrostatic-water MIC management [20].

The superior performance of AgNPs observed here can be rationalized by their multi-modal antibacterial action against SRB. AgNPs release Ag^{+} ions that interact with thiol-rich proteins and respiratory enzymes, destabilize cell membranes, and interfere with DNA/protein functions. In parallel, AgNPs promote oxidative stress via ROS generation and disrupt EPS-mediated SRB biofilms, thereby reducing surface colonization and the cathodic depolarization pathways central to MIC. This mechanistic framework is consistent with our qualitative EIS trends, reduced sulfide-type corrosion products, and minimal pit development on AgNP-treated coupons [21].

AgNP efficacy and persistence in industrial waters depend on medium chemistry. In anaerobic chloride/sulfide-rich environments, AgNPs may transform (e.g., sulfidation), which can change Ag^{+} availability and long-term antimicrobial performance. Literature also reports potential non-target microbial impacts at environmentally relevant concentrations. Therefore, any field deployment should consider optimized dosing and preferably immobilized AgNP coatings or hybrid formulations to limit uncontrolled nanoparticle release. These aspects are highlighted here as limitations and priorities for future industrial-scale validation [22].

In contrast, samples treated with glutaraldehyde presented black iron hydroxide deposits. They showed a corrosion pattern resembling the control sample, which was entirely black due to iron sulfide formation. This highlights glutaraldehyde's inefficacy in eliminating SRB, consistent with studies indicating that certain biocides can inadvertently promote corrosion due to biofilm formation when they fail to eradicate microbial colonies [23-25].

X-ray diffraction (XRD) analysis further supported these findings, as the silver nanoparticle solution did not exhibit the formation of harmful black deposits such as FeS or Fe_3O_4. The predominant phases identified in the silver nanoparticle solution (Fe_2O_3, FeO(OH), and $FeSO_4$(OH)) suggest that sulfate reduction to sulfide was effectively inhibited. This contrasts with glutaraldehyde and control samples, which resulted in the formation of sulfide compounds indicative of active SRB activity.

This contrasts with findings from studies on conventional biocides like chlorine, which, while effective in some contexts, have been shown to form harmful byproducts and exhibit limited efficacy against resistant bacterial spores such as those from Clostridium species [26]. The resistance of these spores to chlorination further underscores the need for alternative antimicrobial strategies, as demonstrated by the efficacy of silver nanoparticles in this study.

The SEM analysis of the steel surfaces revealed varying degrees of pitting corrosion among the samples, with the silver nanoparticle biocide showing minimal pitting. The glutaraldehyde-treated samples displayed significant pitting corrosion and biofilm formation, indicating that glutaraldehyde may create a microenvironment conducive to microbial growth rather than effectively controlling it.

This phenomenon aligns with observations by [27], who noted that biofilm formation can exacerbate corrosion processes when biocides fail to achieve complete microbial eradication. Biofilms on metal surfaces, especially in the case of glutaraldehyde, suggest a counterproductive effect of some biocides in MIC scenarios.

Electrochemical evaluations via LSV and EIS corroborated the physical observations. These results align with studies by [28], which noted silver nanoparticle coatings' exceptional electrochemical stability and corrosion resistance in various environments.

Conversely, the glutaraldehyde sample displayed the lowest charge transfer resistance, indicative of biofilm development and active corrosion processes. This observation reinforces the idea that certain biocides, initially intended to prevent corrosion, may inadvertently facilitate MIC through biofilm promotion. Future research should focus on the synergistic effects of these biocides with protective coatings and explore novel formulations that combine the antimicrobial properties of silver nanoparticles with additional corrosion inhibitors. Such studies could lead to enhanced strategies for preventing corrosion in steel pipelines, thereby extending the lifespan and reliability of critical infrastructure.

3.8. Limitations

The experiments were conducted under static anaerobic conditions; therefore, hydrodynamic shear and flow-assisted mass transfer present during some hydrostatic-testing operations were not reproduced. While static exposure represents the long hold periods typical of hydrostatic tests, flow conditions may influence biofilm detachment and MIC kinetics. Future work should extend the present findings using controlled-flow biofilm reactors (e.g., BioGeorge/flow-loop systems).

4. Conclusions

Most water sources potentially used for hydrostatic testing in West Azerbaijan Province contained Clostridium perfringens. SEM imaging and XRD analysis revealed the deposit types formed under each biocide treatment. The corrosion rates resulting from the use of these biocides were evaluated using electrochemical methods, and the comparison of the obtained graphs was carried out. Ultimately, it was demonstrated that the antibacterial performance of silver nanoparticles surpasses that of conventional chemical biocides. In addition to silver nanoparticles, other metallic nanoparticles such as copper, zinc, and others can be tested, and their efficacy compared with that of silver. The current tests have been conducted at the laboratory scale. It is recommended to evaluate the performance of nanoparticles under real industrial conditions (for example, pipelines in gas fields) and over longer time periods. Additionally, the combination of nanoparticles with anti-corrosion polymeric or epoxy coatings can be studied to simultaneously improve both mechanical strength and microbial resistance.

Data Availability statement

The data that support the findings of this study are available from the corresponding author upon reasonable request. The data are not publicly available due to privacy or ethical restrictions.

Acknowledgements

The authors wish to express their gratitude to Mr. Maleki, representative of Energy Chemical Semnan Company, for his support in supplying industrial biocides.

The authors declare no conflict of interest.

References

1. Lavanya, M., "A brief insight into microbial corrosion and its mitigation with eco-friendly inhibitors", Journal of Bio- and Tribo-Corrosion, 7(3), Article 125, 2021. https://doi.org/10.1007/s40735-021-00563-y
2. Lekbach, Y., Liu, T., Li, Y., et al., "Microbial corrosion of metals: The corrosion microbiome", Advances in Microbial Physiology, 78, pp. 317–390, 2021. https://doi.org/10.1016/bs.ampbs.2021.01.002
3. Procópio, L., "Microbially induced corrosion impacts on the oil industry", Archives of Microbiology, 204(2), Article 138, 2022. https://doi.org/10.1007/s00203-022-02755-7
4. Xu, D., Gu, T., Lovley, D. R., "Microbially mediated metal corrosion", Nature Reviews Microbiology, 21(11), pp. 705–718, 2023. https://doi.org/10.1038/s41579-023-00920-3
5. Knisz, J., Eckert, R., Gieg, L. M., et al., "Microbiologically influenced corrosion—more than just microorganisms", FEMS Microbiology Reviews, 47(5), Article fuad041, 2023. https://doi.org/10.1093/femsre/fuad041
6. Hussein Farh, H. M., Ben Seghier, M. E. A., Taiwo, R., et al., "Analysis and ranking of corrosion causes for water pipelines: A critical review", npj Clean Water, 6(1), Article 65, 2023. https://doi.org/10.1038/s41545-023-00275-5
7. Lv, X., Wang, C., Liu, J., et al., "The microbiologically influenced corrosion and protection of pipelines: A detailed review", Materials, 17(20), Article 4996, 2024. https://doi.org/10.3390/ma17204996
8. Jafari, M., Moghimi, H., Tirandaz, H., et al., "Corrosion behavior of predominant Halodesulfovibrio in a marine SRB consortium and its mitigation using ZnO nanoparticles", Scientific Reports, 14(1), Article 19545, 2024. https://doi.org/10.1038/s41598-024-70654-6

9. Javed, M. A., Neil, W. C., Wade, S. A., "Effect of ferrous sulfate treatment on microbially influenced corrosion of CuNi 70/30 marine pipeline alloy by sulfate reducing bacteria", Environmental Science: Water Research & Technology, 10(10), pp. 2597–2614, 2024. https://doi.org/10.1039/D4EW00382A

10. Ma, T., Wu, T., Gao, K., "Optimization of hydrostatic test plan for pipeline crossing significant elevation difference terrain", International Pipeline Conference, Vol. 88537, p. V001T02A007, 2024. https://doi.org/10.1115/IPC2024-88537-V001T02A007

11. AMPP Annual Conference + Expo, "Rust layer and sulfate reducing bacteria on pipeline steel corrosion in oilfield produced water", C2024-20769, March 2024. https://doi.org/10.5006/c2024-20769

12. Negm, N. A., Altalhi, A. A., Saleh Mohamed, N. E., et al., "Growth inhibition of sulfate-reducing bacteria during gas and oil production using novel Schiff base diquaternary biocides: Synthesis, antimicrobial, and toxicological assessment", ACS Omega, 7(44), pp. 40098–40108, 2022. https://doi.org/10.1021/acsomega.2c04836

13. Farjami, A., Eradati, S., Hamishehkar, H., et al., "Effect of peracetic acid–ultraviolet combination treatment on microbial and endotoxin levels in a pharmaceutical water system", Journal of Water, Sanitation and Hygiene for Development, 12(10), pp. 698–710, 2022. https://doi.org/10.2166/washdev.2022.071

14. Sudarno, S., Wibowo, M. A., Andarini, P., et al., "Mitigating the drinking water crisis in developing regions: A comprehensive evaluation of disinfection technologies", Ecological Engineering & Environmental Technology, 25(5), pp. 85–95, 2024. https://doi.org/10.12912/27197050/184377

15. Guo, K., Wu, Z., Chen, C., et al., "UV/Chlorine process: An efficient advanced oxidation process with multiple radicals and functions in water treatment", Accounts of Chemical Research, 55(3), pp. 286–297, 2022. https://doi.org/10.1021/acs.accounts.1c00269

16. Wang, Y., Zhang, Z., Xia, M., et al., "Mechanism and risk control of chlorine-resistant bacteria in drinking water supply systems: A comprehensive bibliometric analysis", Water, 17(7), Article 956, 2025. https://doi.org/10.3390/w17070956

17. Shaharudin, M. H. A., Rosli, N. R., and Nik Him, N. R., "Assessment of steel corrosion caused by pre-existing microorganism in produced water from an oil and gas facilities and its inhibition using glutaraldehyde", Malaysian Journal of Chemical Engineering and Technology, 4(1), pp. 24–31, 2021. https://doi.org/10.24191/mjcet.v4i1.10946

18. Ezzat, A. O., Aigbodion, V. S., Al-Lohedan, H. A., et al., "Unveiling the corrosion inhibition efficacy and stability of silver nanoparticles synthesized using Anacardium

occidentale leaf extract for mild steel in a simulated seawater solution", RSC Advances, 14(26), pp. 18395–18405, 2024. https://doi.org/10.1039/D4RA02362E

19. Li, C., Cai, Z., Wei, B., et al., "Synthesis of Cu–Ag bimetallic nanoparticle hydrosols and their superior antibacterial performances for control of microbial corrosion by Desulfovibrio desulfuricans biofilm", Advanced Functional Materials, 2025, Article 2500354. https://doi.org/10.1002/adfm.202500354

20. Jafari, M., Moghimi, H., Tirandaz, H., et al. (2024). Corrosion behavior of predominant Halodesulfovibrio in a marine SRB consortium and its mitigation using ZnO nanoparticles. Scientific Reports, 14, 19545. https://doi.org/10.1038/s41598-024-70654-6

21. More, P. R., Pandit, S., De Filippis, A., et al. (2023). Silver nanoparticles: Bactericidal and mechanistic approach against drug resistant pathogens. Microorganisms, 11, 369. https://doi.org/10.3390/microorganisms11020369

22. Sati, A., Ranade, T. N., Mali, S. N., et al. (2025). Silver nanoparticles (AgNPs): Comprehensive insights into bio-synthesis, key influencing factors, multifaceted applications, and toxicity—A 2024 update. ACS Omega, 10, 7549–7582. https://doi.org/10.1021/acsomega.4c11045

23. Xie, P., Xu, X. J., Zhang, Q., et al., "Potent and selective inhibition of sulfate-reducing bacteria by neutral red", Environmental Science & Technology, 59(12), pp. 6115–6125, 2025. https://doi.org/10.1021/acs.est.4c09915

24. Romero-Rodríguez, A., Ruiz-Villafán, B., Martínez-de la Peña, C. F., et al., "Targeting the impossible: A review of new strategies against endospores", Antibiotics, 12(2), Article 248, 2023. https://doi.org/10.3390/antibiotics12020248

25. Kalajahi, S. T., Misra, A., Koerdt, A., "Nanotechnology to mitigate microbiologically influenced corrosion (MIC)", Frontiers in Nanotechnology, 6, Article 1340352, 2024. https://doi.org/10.3389/fnano.2024.1340352

26. Augustyn, W., Chruściel, A., Hreczuch, W., et al., "Inactivation of spores and vegetative forms of Clostridioides difficile by chemical biocides: Mechanisms of biocidal activity, methods of evaluation, and environmental aspects", International Journal of Environmental Research and Public Health, 19(2), Article 750, 2022. https://doi.org/10.3390/ijerph19020750

27. Jones, L., Hanrahan, N., Salta, M., et al., "Evaluating biocide efficacy in mixed-species biofilms: Insights from a dual anaerobic biofilm reactor", npj Materials Degradation, 9(1), Article 97, 2025. https://doi.org/10.1038/s41529-025-00628-0

28. Nedumaran, N., Suresh, N., Gurumoorthy, K., “Fabrication of polydopamine with silver nanoparticles coating on titanium to enhance corrosion resistance: An in vitro analysis”, Journal of Pioneering Medical Sciences, 14, pp. 138–145, 2025. https://doi.org/10.46719/jpms.2025.14.2.0767

Biographies

Dr. Mina Rezapour received her M.Sc. in Physical Chemistry and her Ph.D. in Food Industries (Food Science and Technology) from Urmia University, Urmia, Iran. Her research interests focus on food science and technology and interdisciplinary research addressing industrial and applied challenges in bio-industrial systems.

Dr. Ali Hassanzadeh is an Associate Professor of Physical Chemistry in the Faculty of Chemistry, Urmia University, Urmia, Iran. He received his Ph.D. in Physical Chemistry from Isfahan University of Technology, Isfahan, Iran. His research interests focus on the physical chemistry of materials, nanomaterials and nanoparticles, surface/solution electrochemistry, and corrosion-related applications. He has published research articles in these areas and is affiliated with Urmia University and its Nanotechnology Research Center.

Dr. Nima Shaykh-Baygloo is an Associate Professor in the Department of Biology, Urmia University, Urmia, Iran. He received his Ph.D. and M.Sc. in Microbiology from the University of Isfahan, Isfahan, Iran. His research interests focus on applied and environmental microbiology, microbial biofilms, and microbial–material interactions relevant to bio-industrial systems. He has published research articles in these areas and is actively involved in teaching and research at Urmia University.

List of Figures

List of Tables

Figures

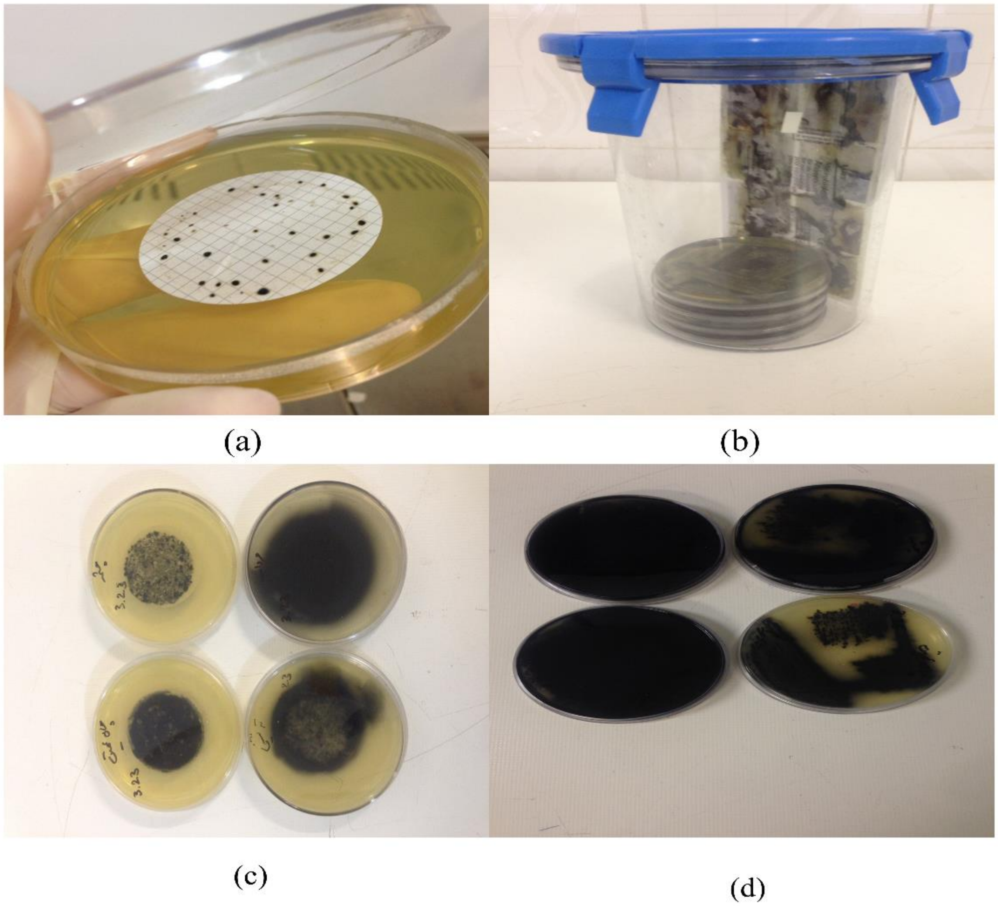

Figure 1. *Clostridium perfringens* colonies grown on TSC agar: **(a)** Typical colonies on TSC agar, **(b)** Anaerobic jar, **(c, d)** Positive growth in tested water samples

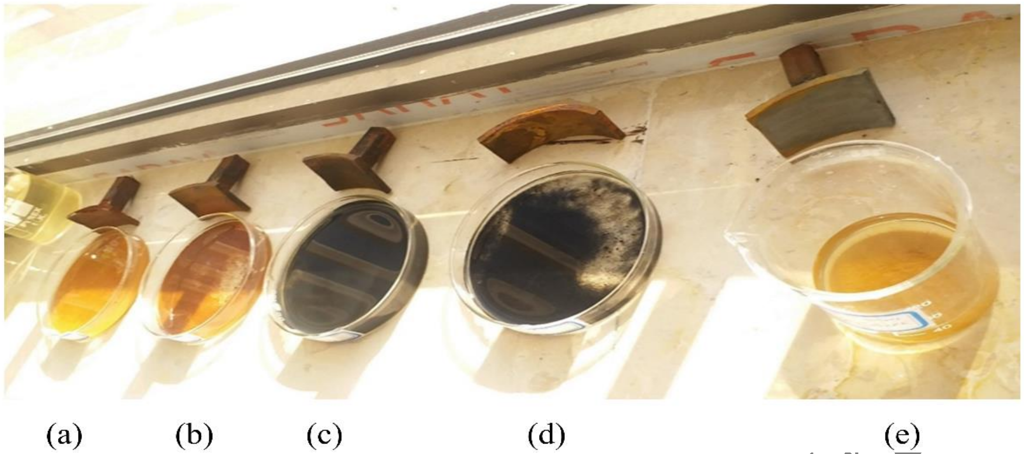

Figure 2. Sediments resulting from corrosion of carbon steel pipes in biocide-treated and control samples: **(a)** Mixture, **(b)** Isothiazolinone, **(c)** Glutaraldehyde, **(d)** Blank, **(e)** AgNPs

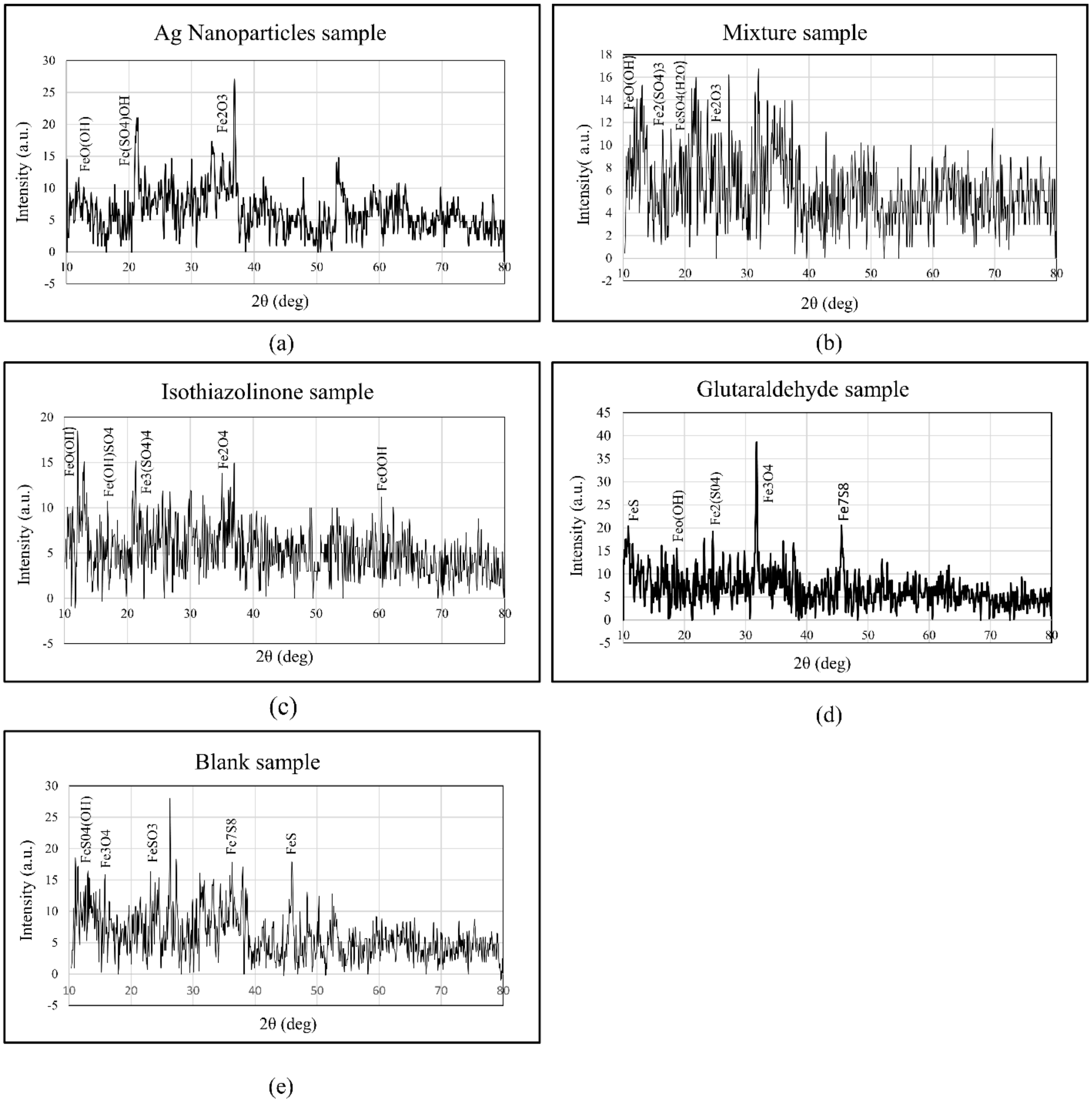

Figure 3. XRD pattern analysis of sediment deposits from biocide-treated and control samples.

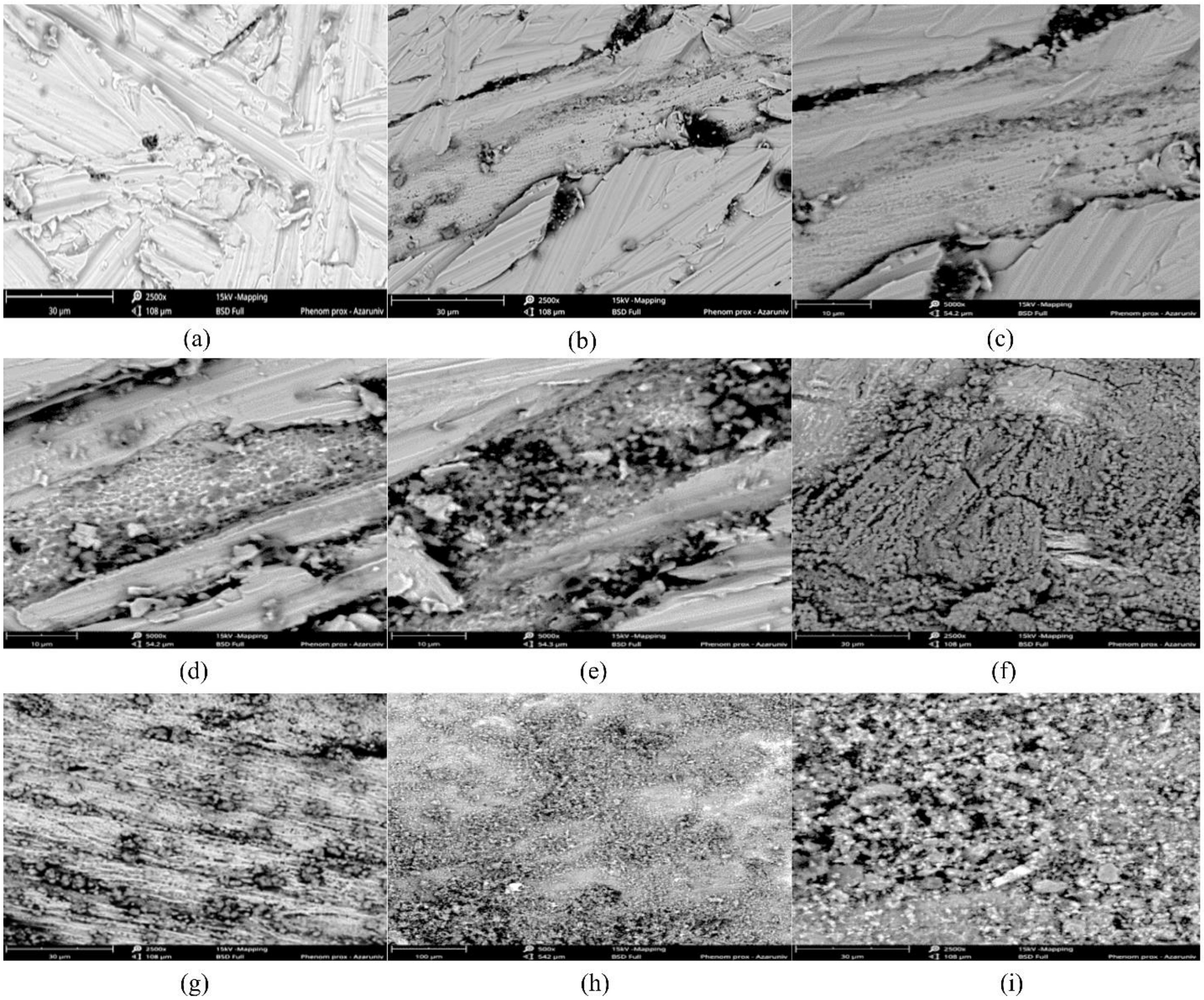

Figure 4. SEM micrographs of carbon steel coupon surfaces after 40-day exposure to SRB-inoculated thioglycollate medium under different biocide treatments: (a) AgNPs, (b) Mixture-1, (c) Mixture-2, (d) Isothiazolinone-1, (e) Isothiazolinone-2, (f) Glutaraldehyde-1, (g) Glutaraldehyde-2, (h) Blank-1, and (i) Blank-2.

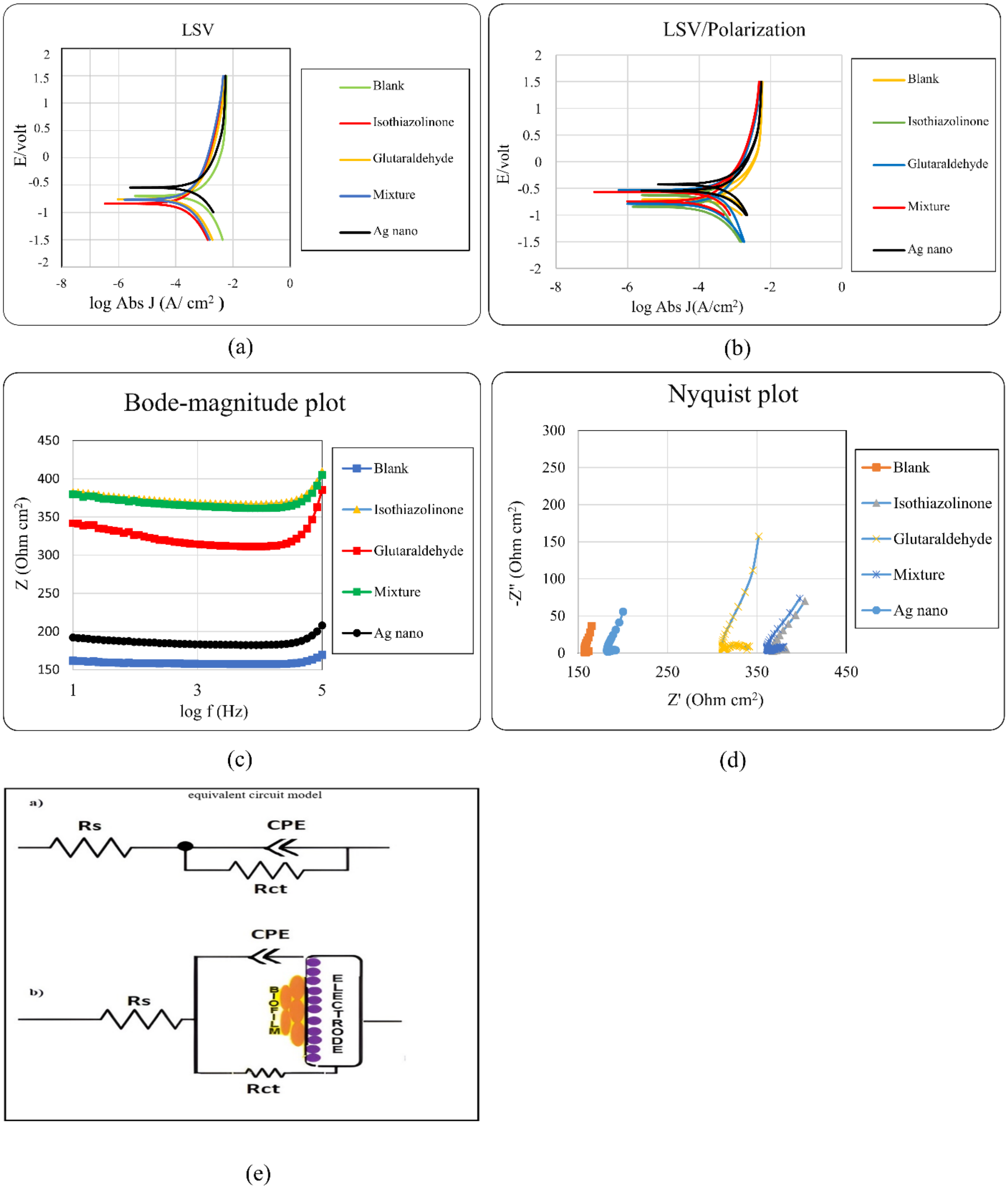

Figure 5. Electrochemical characterization of steel samples (LSV, Nyquist and Bode plots) and the equivalent circuit model used for EIS fitting.

Tables

Table 1. Sampling sites, depths, and characteristics of water samples in the Urmia region.

Sampling Sites	**Sampling Depth (cm)**	**Sample Characteristics**	**Location Coordinates**
Urmia and Surroundings 1	20-25	Low to medium turbidity	45° 0' 44.73" E, 37° 39' 10.80" N
Urmia and Surroundings 2	20-25	Low to medium turbidity	45° 6' 13.9" E, 38° 51' 50" N
Urmia and Surroundings 3	20-25	Low to medium turbidity	45° 6' 25.5" E, 38° 51' 48.6" N
Urmia and Surroundings 4	20-25	Low to medium turbidity	45° 6' 17.8" E, 38° 51' 50.3" N
Urmia and Surroundings 5	20-25	Low to medium turbidity	45° 5'30.1" E, 38° 51'34.9" N

Table 2. Fitting results of the polarization curves of steel samples using the Butler–Volmer equation.

Parameter	Unit	Blank	Isothiazolinone sample	Glutaraldehyde sample	Mixture sample	Ag-nano
βa	*mV/decade*	1880.7	1619.1	1399	1370.2	946.17
βc	*mV/decade*	1797.4	1290	1329	1274	517.09
Jcorr.	A/cm^2	0.0018799	0.00046782	0.000587	0.0004446	0.00058979
Ecorr.	*volt*	-0.69828	-0.803807	-0.75969	-0.76658	-0.75217
Rp	$\Omega \cdot cm^2$	206.45	658.19	503.41	636	228.1
*CR*1E-10*	*mpy*	8.77287	2.18316	2.73933	2.0748	2.75235

Table 3. CV data results

	Blank	Isothiazolinone	Glutaraldehyde	Isothiazolinone + Bronopol	Ag-nano
$E_{corr./volt}$	-0.7095	-0.8432	-0.7870	-0.7437	-0.5435
$E_{diffusion/volt}$	-0.0283	-0.1229	+0.0161	-0.1992	+0.0253
$E_{repass./volt}$	-0.5508	-0.6259	-0.5307	-0.5654	-0.4190
Hysteresis	negative	negative	negative	negative	negative

Table 4. EIS fitted parameters of carbon steel in SRB medium under different biocide treatments

	Blank	Isothiazolinone	Glutaraldehyde	Isothiazolinone +Bronopol	Ag-nano
$R_{s/Ohm\ cm^2}$	156.6	362.9	307.5	353.9	178.6
CPE-T (C_{dl}) F/cm^2	0.042	0.0046	0.0007	0.015	0.015
CPE-P	0.337	0.388	0.560	0.205	0.277
$R_{ct/Ohm\ cm^2}$	710020	35.68	42.8	$2.58\times10^{+7}$	42.55
chi-square	$2.6896\times10^{+20}$	13.98663	4.887844	2.4006410^{+24}	117.6598

Table 5. Corrosion inhibition efficiency of the tested biocides based on LSV-derived i_corr values.

	Isothiazolinone	Glutaraldehyde	Isothiazolinone+Bronopol	Ag-nano
Yield based on LSV	24.88	74.52	75.74	67.34